A COMPREHENSIVE MODEL FOR EVALUATING THE PERFORMANCE OF PROTON EXCHANGE MEMBRANE FUEL CELLS

Faycel Khemili *, Mustapha Najjari °, Sassi Ben Nasrallah*

* Laboratoire d'Etudes des Systèmes Thermiques et Energétiques, Ecole Nationale d'Ingénieurs de Monastir, Avenue Ibn El Jazzar, 5019 Monastir, Tunisie
° Faculté des Sciences de Gabès, Cité Riadh, Zirig 6072 Gabès, Tunisia

ABSTRACT

Modeling plays an important role in the development of Proton Exchange Membrane Fuel Cell (PEMFC), because it allows a better comprehension of the parameters affecting the fuel performances. PEMFC performances are strongly related to the mechanisms of mass transfer in the stack. The objective of this study is to develop a comprehensive model describing the transport phenomena in the cell and these influences on the fuel performances. First, we present the electrochemical model that takes into account the thermodynamic open circuit voltage and different voltage losses. Second, we present gas diffusion in porous electrodes, water diffusion and electro-osmotic transport through the polymeric membrane. The solutions of the mass transfer equations are used to calculate the fuel cells performances at different operating conditions.

1. INTRODUCTION

In the fifteen previous years, fuel cells have received significant attention and they are expected to play an important role in future power generation facilities. Fuel cells are part of a promising environmentally friendly electricity generating technology, which can be used for stationary and mobile applications. The existing categories of fuel cells are mainly based on the type of electrolyte and the operating temperature. The choice of the operating region leads to different characteristics for the system regarding its profitability, effectiveness and safety. Life time and reliability appear to be important elements to successfully achieve the commercialization of such systems. In recent years there is an increasing interest in utilizing proton exchange membrane fuel cells PEMFC for small portable or stationary applications. PEMFC utilizes hydrogen and air to produce electricity and water, has high power density and uses a solid electrolyte, it has also a long stack life, as well as a low degradation due to corrosion.

Within a PEMFC several coupled physical phenomena occur. The electrochemical reactions at the interface electrode/membrane generate heat (heat transfer), produce water at the cathode and consume reactants (mass transfer). And it's also impose a flux of protons across the membrane and a transfer of electrons from one electrode to the other (charge transport). These three types of transport are coupled and influence the performance of the fuel cell.

To achieve optimal fuel cell performances, it is essential to have an adequate water balance to ensure that the membrane remains hydrated for sufficient proton conductivity and an adequate transport of species through the electrodes to the reaction sites. Understanding the mass transfer phenomena within the Membrane Electrodes Assembly (MEA) is a key issue to avoid membrane dehydration and to ensure that a sufficient reactant quantity reaches the reactions sites which improves the PEMFC performances.

In the last decade, researchers have developed several mathematical models to describe several transport mechanisms in Membrane Electrodes Assembly.

Bernardi and Verbrugge [1] modeled the water transport and electrochemical behavior of the cell with the restriction of a fully hydrated membrane. Springer et al. [2] described the electro-osmotic drag and back diffusion mechanisms of the water transport and the net water transport coefficient in the membrane without the electrochemical reaction in the catalyst layer. The first model used to predict cell voltage as a function of current density was developed by Amphlett [3], which is based on Nernst and Tafel equations. It considered all physical parameters in the system (pressure of oxygen and hydrogen, temperature, etc).

Prodip K. Das et al. [4] presented a one-dimensional analytical solution of liquid water transport across the cathode catalyst layer (CCL) which is derived from the fundamental transport equations. The objective of his study is to investigate the water transport in the CCL of a PEMFC. The effect of CCL wettability on liquid water transport and the effect of excessive liquid water on reactant transport and cell performance have been investigated

Najjari et al. [5] have numerically investigated the effects of the flooding of the gas diffusion layer (GDL), as a result of liquid water accumulation, on the performance of PEMFC.

Khemili et al. [6] developed a two-phase flow and mass transport in the porous cathode of a Proton Exchange Membrane Fuel cell (PEMFC). A model, based on the model of the separate-phase-flow is used to solve the mass

conservation equations. This model is used to test the effect of the presence of liquid water on the mechanisms of transport in the porous cathode and its influence on the performance of the fuel cell.
Khemili et al. [7] developed a transient two-dimensional model to study the mass transfer inside the gas-channel-flow and the porous cathode of a Proton Exchange Membrane Fuel Cell (PEMFC). A unified approach is used to model both the gas-channel-flow and the porous cathode. An analytic solution of velocity in the gas-channel-flow is used.
Electrochemical responses of the PEMFC have been analysed and discussed. Profiles of oxygen concentration, water concentration and cathode overpotential are presented.
A number of empirical models have been developed for fuel cells. The model of Chamberlin and Kim [8] describes the cell voltage depending on the current density, with many parameters which accounted for thermodynamic, kinetic, ohmic and mass transfer effects. Many of the models have limited use as they fail to show the real effect of system variables on performance [8,9,10].

The aim of the present study is to develop a comprehensive model which incorporates water transport in the membrane and mass transfer in the electrodes, and to investigate the effect of many operating conditions on the fuel cell performance.

2. MATHEMATICAL MODEL

The schematic diagram of PEMFC is shown in Fig.1. A PEMFC consists of a porous anode, a membrane and a porous cathode.

At the anode, the hydrogen molecule is split into hydrogen protons and electrons under the action of catalyst according to the following reaction:

$$H_2 \rightarrow 2H^+ + 2e^- \quad (1)$$

The hydrogen protons permeate across the polymer membrane to the cathode. The electrons flow through an external circuit and produce electric power. Oxygen, usually in the form of air, is supplied to the cathode and combines with electrons and hydrogen protons to produce water:

$$\frac{1}{2}O_2 + 2H^+ + 2e^- \rightarrow H_2O \quad (2)$$

The overall reaction in a PEMFC can be written as:

$$H_2 + \frac{1}{2}O_2 \rightarrow H_2O \quad (3)$$

The produce of this process are water, electricity and heat.

2.1. Electrochemical models

The output fuel cell voltage U is the difference between the thermodynamic open circuit-voltage E_{thermo} and the activation concentration overpotentials $\eta_{act,con}$ and the ohmic overpotential η_{ohm} :

$$U = E_{thermo} - \eta_{act,con} - \eta_{ohm} \quad (4)$$

2.1.1. Thermodynamic open circuit voltage

The maximum amount of electrical energy generated in a fuel cell corresponds to Gibbs free energy, $\Delta G(T,P)$, of the above reaction:

$$W_{ele} = -\Delta G \quad (5)$$

The Gibbs free energy $\Delta G(T,P)$ is related to the enthalpy and the entropy by:

$$\Delta G = \Delta H - T\,\Delta S \quad (6)$$

Assuming that hydrogen, oxygen and water vapor are ideal gazes, $\Delta G(T,P)$ can be calculate with the following expression:

$$\Delta G(T,P) = \Delta G(T,P_0) + RT \ln\left(P_{H_2}\left(P_{O_2}\right)^{0.5}\right) \quad (7)$$

Where P_i the partial pressure of specie i, $\Delta G(T,P_0)$ the reaction entropy at standard pressure P_0 and R the gas constant.

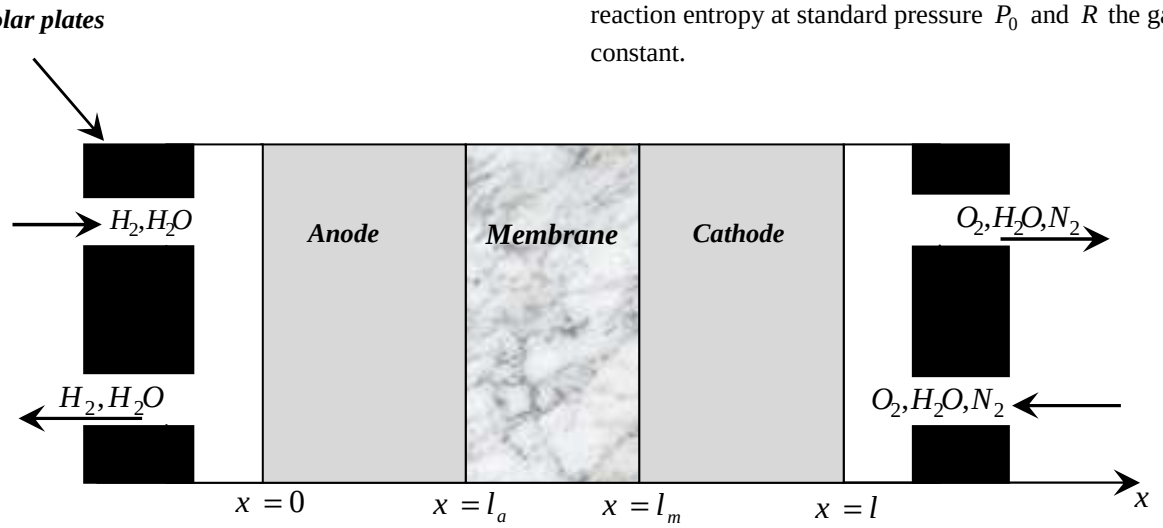

Figure 1. Schematic description of the PEMFC single cell

$\Delta G\left(T,P_0\right)$ is determined by the following equation:

$$\Delta G\left(T,P_0\right) = -n\,F\,E\left(T,P_0\right) \quad (8)$$

The thermodynamic voltage at standard pressure $E\left(T,P_0\right)$ can be calculated as follows:

$$E\left(T,P_0\right) = E\left(T_0,P_0\right) + \left(T - T_0\right)\frac{\Delta S^0}{2F} \quad (9)$$

Where T_0 is the standard temperature (298.15 K) and $E\left(T_0,P_0\right)$ is the standard thermodynamic voltage. $E\left(T_0,P_0\right) = 1.229V$ if water product in liquid phase and $E\left(T_0,P_0\right) = 1.18V$ if water product in vapor phase.

Substituting Eqs. (7) and (9) into Eq. (8) yields:

$$E_{th} = E\left(T_0,P_0\right) + \left(T - T_0\right)\frac{\Delta S^0}{2F} + \frac{RT}{2F}\ln\left(P_{H_2}\left(P_{O_2}\right)^{0.5}\right) \quad (10)$$

Where $\frac{\Delta S^0}{2F}$ is the standard entropy of reaction (2):

$$\frac{\Delta S^0}{2F} = \begin{cases} -0.85.10^{-3}V.K^{-1} & \text{if water product in liquid phase} \\ -0.23.10^{-3}V.K^{-1} & \text{if water product in vapor phase} \end{cases} \quad (11)$$

Assuming water is produced in liquid phase, Eq. (6) becomes:

$$E_{th} = 1.229 - 0.85.10^{-3}\left(T - T_0\right) + \frac{RT}{2F}\ln\left(P_{H_2}\left(P_{O_2}\right)^{0.5}\right) \quad (12)$$

2.1.2. Activation overpotential

The activation overpotential is caused by the slowness of the electrochemical reaction requiring activation energy to occur. A portion of the voltage generated is lost because of the chemical reaction that transfers the electrons to or from the electrodes. The activation polarization can be expressed by the flowing equation [11]:

$$I = I_{0,ele}\left[\exp\left(\frac{\alpha_a^{ele}F}{RT}\eta_{act,ele}\right) - \exp\left(-\frac{\alpha_c^{ele}F}{RT}\eta_{act,ele}\right)\right] \quad (13)$$

Where $I_{0,ele}$ is the exchange current density at an electrode, α_a^{ele} and α_c^{ele} are the anodic and cathodic transfer coefficients, respectively.

Assuming that the transfer coefficients on an electrode are equal, the expression of activation overpotential on an electrode becomes:

$$\eta_{act,ele} = \frac{RT}{\alpha^{ele}F}sh^{-1}\left[\frac{I}{2I_{0,ele}}\right] \quad (14)$$

The total activation overpotential in the cell is the sum of the anode and the cathode contributions:

$$\eta_{act} = \eta_{act,a} + \eta_{act,c} = \frac{RT}{\alpha^a F}sh^{-1}\left[\frac{I}{2I_{0,a}}\right] + \frac{RT}{\alpha^c F}sh^{-1}\left[\frac{I}{2I_{0,c}}\right] \quad (15)$$

The exchange current density at the cathode I_0^c is dependent on the temperature and can be modeled by the following equation (Hyunchul et al. [12]):

$$I_{0,c} = \gamma_c I_{0,ref}^c \exp\left(16456\left(\frac{1}{T} - \frac{1}{353}\right)\right) \quad (16)$$

Where $I_{0,ref}^c$ is the cathode reference exchange current density and γ_c the roughness factor.

The exchange current density at the anode $I_{0,a}$ is taken constant [13].

2.1.3. Concentration overpotential

During the reaction process, concentration gradients can be formed due to mass diffusions from the flow channels to the reaction sites. At high current densities, slow transportation of reactants to the reaction sites is the main reason for the concentration voltage drop. Any water film covering the catalyst surfaces at the anode and cathode can be another contributor to this voltage drop. The concentration overpotential in the fuel cell is the sum of the anode and cathode contributions:

$$\eta_{con} = \eta_{con,a} + \eta_{con,c} = \frac{RT}{\alpha^a F}\ln\left(\frac{C_{ref}^{H_2}}{C_{H_2}^*}\right) + \frac{RT}{\alpha^c F}\ln\left(\frac{C_{ref}^{O_2}}{C_{O_2}^*}\right) \quad (17)$$

Where C_{ref}^i and C_i^* are the reference concentration and the concentration of specie i in the membrane/electrode interface.

In a fuel cell, the oxygen reduction is much slower than the hydrogen oxidation. It follows that the anode overpotential is negligible compared to the cathode overpotential:

$$\eta_{act} + \eta_{con} = \frac{RT}{\alpha_c F}\ln\left(\frac{I}{I_{0,c}}\right) + \frac{RT}{\alpha_c F}\ln\left(\frac{C_{ref}^{O_2}}{C_{O_2}^*}\right) \quad (18)$$

2.1.4. Ohmic overpotential

The ohmic overpotential represents a measure of the ohmic voltage drop associated with the conduction of the protons through the solid membrane and electrons through the internal electronic resistances:

$$\eta_{ohm} = rI = r^{ele}I + r^{ion}I \quad (19)$$

The resistance to electron transfer r^{ele} is considered constant in the temperature range covered by this study.

The ionic resistance r^{ion}, can be expressed as a function of thickness of the electrolyte membrane l_m and the ionic conductivity σ_m:

$$r^{ion} = \int_0^{l_m}\frac{dx}{\sigma_m\left(x\right)} \quad (20)$$

The ionic conductivity is a function of many variables: cell temperature, degree of humidification of the membrane and the water content of the membrane λ.

The membrane conductivity is obtained as shown below (Springer et al. [2]):

$$\sigma_m = 10^{-2} \times (0.519\lambda - 0.326) \exp\left(1263\left(\frac{1}{303} - \frac{1}{T}\right)\right) \quad (21)$$

2.1.5. Output voltage

Considering the above development, the output voltage can be expressed by:

$$\begin{aligned} U &= 1.229 - 0.85.10^{-3}(T - T_0) + \frac{RT}{2F}\ln\left(P_{H_2}\left(P_{O_2}\right)^{0.5}\right) \\ &- rI - \frac{RT}{\alpha_c F}\ln\left(\frac{I}{I_{0,c}}\right) - \frac{RT}{\alpha_c F}\ln\left(\frac{C_{ref}^{O_2}}{C_{O_2}^{*}}\right) \end{aligned} \quad (22)$$

2.5.6. Output power

Once the output voltage of the stack is determined for a given output current, the gross output power is found as:

$$W = U.I \quad (23)$$

In order to calculate the fuel cell performances, the molar concentrations of species and water content in the membrane need to be determined. In the following section, a mathematical approach is presented for building a transport model for a PEMFC.

2.2. Mass transfer in the Membrane Electrodes Assembly

2.2.1. Transport in the porous electrode

In a gas mixture consisting of species, most of the models encountered in the literature use the Stefan Maxwell equations to describe the diffusion of gas in the porous electrodes [14]:

$$\frac{dy_k}{dx} = \sum_{k,i \neq k} \frac{1}{c}\left(\frac{y_k N_i - y_i N_k}{D_{k,i}^{eff}}\right) \quad (24)$$

And $$\sum_k y_k = 1$$

Where y_k and N_k represent, respectively, the mole fraction and the molar flux densities of species k . $c = \frac{P}{RT}$ the molar concentration of the gas mixture

With

$$k, i = \begin{cases} H_2, H_2O & \text{at the anode side} \\ O_2, H_2O, N_2 & \text{at the cathode side} \end{cases}$$

The effective diffusion coefficients $D_{k,i}^{eff}$ can be evaluated using Bruggeman's correction [14]:

$$D_{k,i}^{eff} = \varepsilon^{\frac{3}{2}} D_{k,i} \quad (25)$$

Where ε is the porosity of the porous electrode.

At the anode side, the diffusion of species can be expressed by the flowing system equations:

$$\begin{cases} \dfrac{dy_{H_2}}{dx} = \dfrac{1}{cD_{H_2,H_2O}^{eff}}\left(y_{H_2}\left(N_{H_2O}^{a} + N_{H_2}\right) - N_{H_2}\right) \\ y_{H_2} + y_{H_2O}^{a} = 1 \end{cases} \quad (26)$$

Assuming that $N_{H_2O} + N_{H_2} \neq 0$, the integrating of the above equation leads to:

$$\begin{aligned} y_{H_2}(x) &= \frac{N_{H_2}}{N_{H_2} + N_{H_2O}^{a}} + \\ &\left(y_{H_2}^{in} - \frac{N_{H_2}}{N_{H_2} + N_{H_2O}^{a}}\right)\exp\left(\frac{N_{H_2O}^{a} + N_{H_2}}{cD_{H_2,H_2O}^{eff}}x\right) \end{aligned} \quad (27)$$

Where $y_{H_2}^{in}$ is the hydrogen molar concentration in the anode channel:

$$\begin{aligned} y_{H_2}^{in} &= 1 - RH_a\frac{P_{sat}}{p} \\ y_{H_2O}^{a,in} &= RH_a\frac{P_{sat}}{p} \end{aligned} \quad (28)$$

Where RH_a is the relative humidity at the anode channel.

At the cathode side, the diffusion of species can be expressed by the flowing system equations:

$$\begin{cases} \dfrac{dy_{O_2}}{dx} = \dfrac{N_{O_2} + N_{H_2O}^{c}}{cD_{O_2,H_2O}^{eff}}y_{O_2} + \\ \quad \left(\dfrac{1}{cD_{O_2,H_2O}^{eff}} - \dfrac{1}{cD_{O_2,N_2}^{eff}}\right)N_{O_2}y_{N_2} - \dfrac{N_{O_2}}{cD_{O_2,H_2O}^{eff}} \\ \dfrac{dy_{N_2}}{dx} = \dfrac{1}{c}\left(\dfrac{N_{N_2}}{D_{O_2,N_2}^{eff}} + \dfrac{N_{H_2O}^{c}}{D_{O_2,N_2}^{eff}}\right)y_{N_2} \\ y_{O_2} + y_{H_2O}^{c} + y_{N_2} = 1 \end{cases} \quad (29)$$

Assuming that $N_{O_2} + N_{H_2O} \neq 0$, the integrating of the above equation between the anode channel and the catalyst surface, leads to:

$$\begin{aligned} y_{O_2}(x) &= \left[y_{O_2}^{in} - \frac{N_{O_2}}{k_c cD_{O_2,H_2O}^{eff}} - k_H y_{N_2}^{in}\frac{N_{N_2}}{k_n - k_c}\right]\exp\left(k_c(x - l_c)\right) \\ &+ y_{N_2}^{in}k_H\frac{N_{O_2}}{k_n - k_c}\exp\left(k_c(x - l_c)\right) + \frac{N_{O_2}}{cD_{O_2,H_2O}^{eff}}\frac{1}{k_c} \end{aligned} \quad (30)$$

Where:

$$k_c = \frac{N_{O_2} + N_{H_2O}^{c}}{cD_{O_2,H_2O}^{eff}}\ ,\ k_n = \frac{N_{H_2O}^{c}}{cD_{N_2,H_2O}^{eff}} + \frac{N_{O_2}}{cD_{O_2,N_2}^{eff}}\ ,$$

$$k_H = \frac{1}{cD_{O_2,H_2O}^{eff}} - \frac{1}{cD_{N_2,O_2}^{eff}}$$

$y_{O_2}^{in}$ and $y_{N_2}^{in}$ are the molar concentrations of oxygen and nitrogen in the gas channels:

$$y_{O_2}^{in} = 0.21\left(1 - RH_c \frac{P_{sat}}{p}\right)$$
$$y_{N_2}^{in} = 0.79\left(1 - RH_c \frac{P_{sat}}{p}\right) \quad (31)$$
$$y_{H_2O}^{c,in} = HR_c \frac{P_{sat}}{p}$$

Where RH_c is the relative humidity at the cathode channel.

The molar flux densities of hydrogen and oxygen at the anode and at the cathode, respectively, are given by the Faraday's low:

$$N_{H_2} = \frac{I}{2F} \ , \ N^{O_2} = \frac{I}{4F} \quad (32)$$

The electrolyte membrane being impervious to gases, hydrogen and oxygen only flows from gas channels to the anode and to the cathode, respectively. Only water can pass through the membrane. Fluxes are considered positive in the x direction:

In the anode:

$$N_{H_2O}^{a} = N_{H_2O}^{m} \quad (33)$$

In the cathode:

$$N_{H_2O}^{c} = \frac{I}{2F} + N_{H_2O}^{m} \quad (34)$$

2.2.2. Transport in the membrane

Water transport inside the membrane is represented by the change in membrane water content, λ, defined as the number of water molecules held per sulphonic acid group $\left(SO_3^-\right)$.

$$\lambda = \frac{EW}{\rho_{dry}} c_{H_2O} \quad (35)$$

Where EW is the equivalent weight which is the dry membrane weight per mole of sulfonate group, ρ_{dry} is the density of dry polymer and c_{H_2O} the local concentration of water in the membrane.

The key equation in the membrane is the transport of the water. There are two distinct mechanisms that govern the transport of water in the membrane: electro-osmotic drag due to protons from anode to cathode; diffusion due to a concentration gradient inside the membrane. When the current is drawn from the cell, protons move from anode to cathode through the membrane and water molecules are carried by protons. This process is called the electro-osmotic drag and average number of water molecules carried by one proton is called electro-osmotic drag coefficient.

When the water concentrations are different at the anode and the cathode there is a concentration gradient which drives the diffusion of the water molecules from higher concentration sites to lower concentration sites.

The total water flux through the membrane is the sum of electro-osmotic and diffusive fluxes:

$$N_{H_2O}^{m} = \frac{2.5}{22}\frac{I}{F}\lambda - D_{H_2O}^{m}\frac{\rho_{dry}}{EW}\frac{\partial \lambda}{\partial x} \quad (36)$$

Denoting λ_a and λ_c the water contents at the membrane/cathode and membrane/anode interfaces, respectively, the water content λ and water flux through the membrane are given by:

$$\lambda(x) = \lambda_a + (\lambda_c - \lambda_a)\frac{1-\exp(k_m)x}{1-\exp(k_m l_m)} \quad (37)$$

And

$$N_{H_2O}^{m} = \frac{2.5}{22}\frac{I}{F}\left(\lambda_a + \frac{\lambda_c - \lambda_a}{1-\exp(k_m l_m)}\right) \quad (38)$$

With $$k_m = \frac{EW}{D_{H_2O}^{m}\rho_{dry}}\frac{2.5}{22}\frac{I}{F}$$

λ_a and λ_c depend on the relative humidity of the gas mixtures at the electrode/membrane interfaces according to the sorption isotherms. However, in the literature, the relationships frequently chosen to describe the sorption isotherms in the membrane are [15-16]:

$$\lambda_{30°C} = 0.043 + 17.81a - 39.85Ra^2 + 36a^3 \quad (39)$$

$$\lambda_{80°C} = 0.3 + 10.8a - 16a^2 + 14a^3 \quad (40)$$

Where a the activity of water vapor defined by:

At the anode/membrane interfaces:

$$a = y_{H_2O}^{a}\frac{P}{P_{sat(T)}} \quad (41)$$

At the anode/membrane interfaces:

$$a = y_{H_2O}^{c}\frac{P}{P_{sat(T)}} \quad (42)$$

where the saturation pressure, $P_{sat(T)}$

The saturation pressure $P_{sat(T)}$ can be evaluated using the following correction [17]:

$$\log_{10}\left(P_{H_2O}^{sat}\right) = -2.1794 + 0.02953(T - 273.15) - 9.1837\times10^{-5}(T-273.15)^2 + 1.4454\times10^{-7}(T-273.15)^3 \quad (43)$$

The sorption curves found in [15,16] at T = 30°C and 80°C are presented in figure 2.

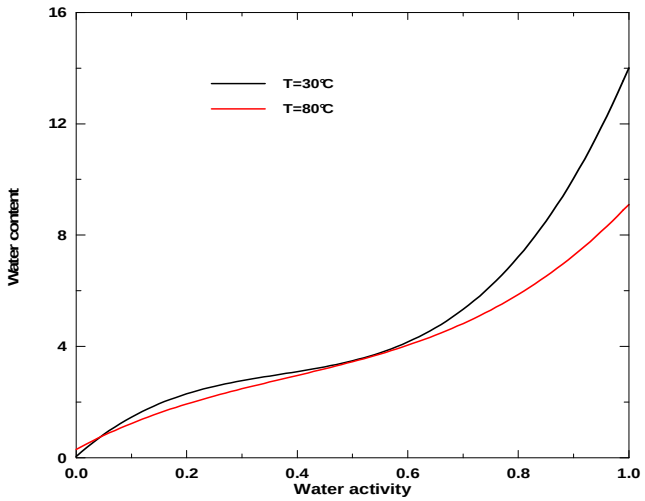

Figure.2. The sorption curves

3. RESULTAS AND DISCUSSIONS

The solutions of the equations of mass transport in the Membrane Electrodes Assembly are coupled. Indeed, the water flux in the membrane is unknown. An iterative proedure is used: first, a water flux is arbitrarily chosen to solve equations of mass transport which allows us to evaluate the compositions of gases in the electrodes. Second, the sorption isotherms are used to calculate the water content at the interface membrane/electrodes. Third, we calculate the water flux in the membrane. The calculation is repeated until equality between the arbitrary water flux and water flux into the membrane is achieved. The input data for parameters applied in this study are listed in table 1.

Parameter	Symbol	value
Cathode thickness	$l_c\,(m)$	230×10^{-6}
Anode thickness	$l_a\,(m)$	230×10^{-6}
Membrane thickness	$l_m\,(m)$	175×10^{-6}
Equivalent oxygen diffusivity	$D^{eff}_{O_2,H_2O}\left(m^2.s^{-1}\right)$	$0,34.10^{-4}$
Equivalent hydrogen diffusivity	$D^{eff}_{H_2,H_2O}\left(m^2.s^{-1}\right)$	$3.5.10^{-5}$
Equivalent water diffusivity in the membrane	$D^{m}_{H_2O}\left(m^2.s^{-1}\right)$	3.10^{-10}
The equivalent weight	$EW\ \left(kg.mol^{-1}\right)$	1.1
Density of dry polymer	$\rho_{dry}\left(kg.m^{-3}\right)$	2020

Table 1: Physical properties and geometrical parameters used in numerical simulations

3.1. Distribution of water content in the membrane

In Fig. 3(a) and 3(b), water content in the membrane at different current densities and at two operating conditions is presented. The water content decreases with the increasing current density. For high current densities, the water transport from the anode to the cathode by electro-osmotic drag exceeds the water transport by back diffusion from the cathode to the anode. This leads to the eventual dry out of the membrane. The water profiles then show a curvature. The water back diffusion is limited by the membrane pores which shrink due to dehydration. Therefore, the water transport by back diffusion is not enough to prevent membrane dehydration. Humidified anode and cathode streams are needed to avoid the membrane dehydration, particularly at high current densities. At low current densities, the profile of water content in the membrane approaches the linear profile imposed by the diffusive flux.

When the anode is not sufficiently humidified, the membrane is well hydrated (fig. 3(a)). However, if the anode is more humidified, the membrane may dry out more when the current density increases. The amount of water is higher for the cathode side due to the domination of water transport by electro-osmotic drag and water generation by reaction. The mean water content in the membrane is higher in the case 3.a, then in the case 3.b

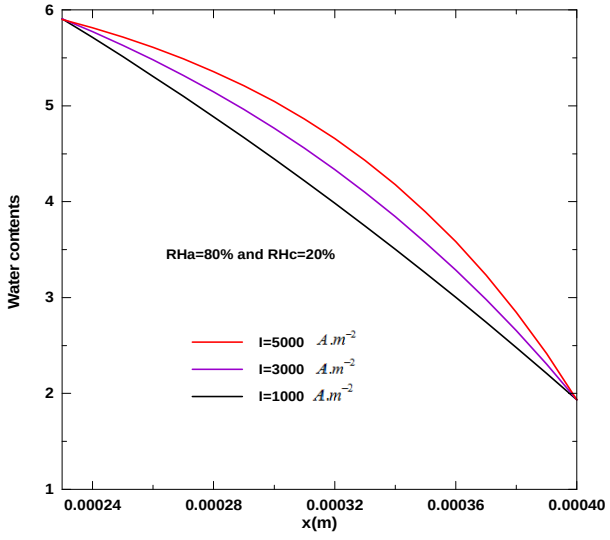

(a)

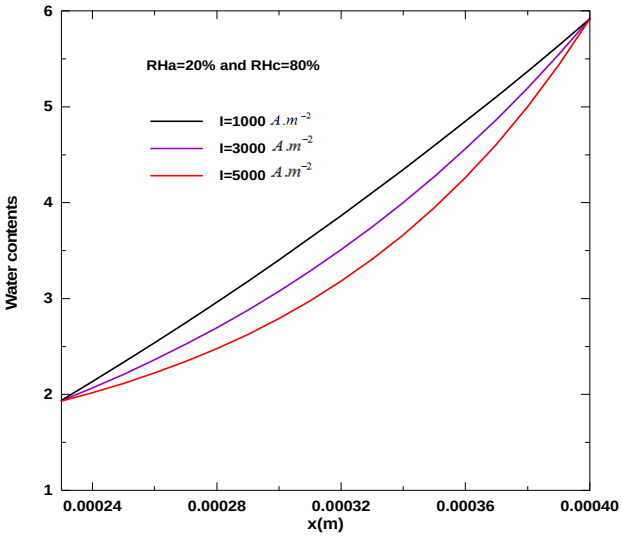

(b)

Figure 3. Water content along the membrane for different operating conditions and for different current densities

3.2. Distribution of oxygen molar fractions

Figure 4 shows the mole fraction profiles of oxygen in the cathode for three different current densities. It can be seen that the mole fraction vary linearly within the cathode. This is because the very small thickness of the cathode and purely diffusive transport without production or consumption of species and without liquid phase. The mole fraction of oxygen decreases and molar water fraction increases when approaching the cathode/membrane interface. This phenomenon is more significant at higher current density (fig. 5). Indeed, in the case of large current density, the electrochemical reaction rate gets faster and much more oxygen is needed to react and more water is generated. Therefore, the oxygen diffusion rate must follow the reaction rate

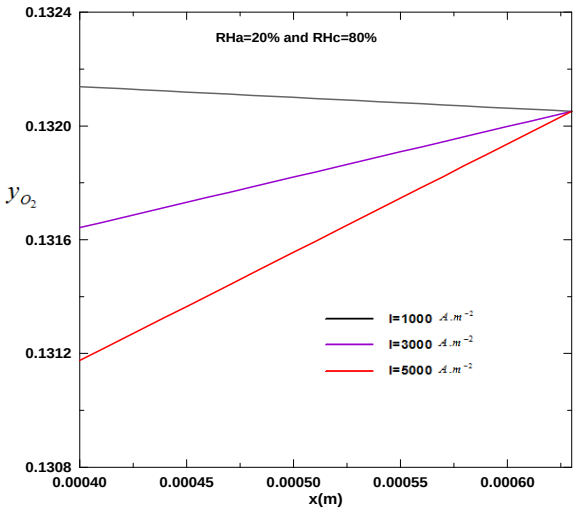

Figure 4. Oxygen mole fraction along the cathode for different current densities

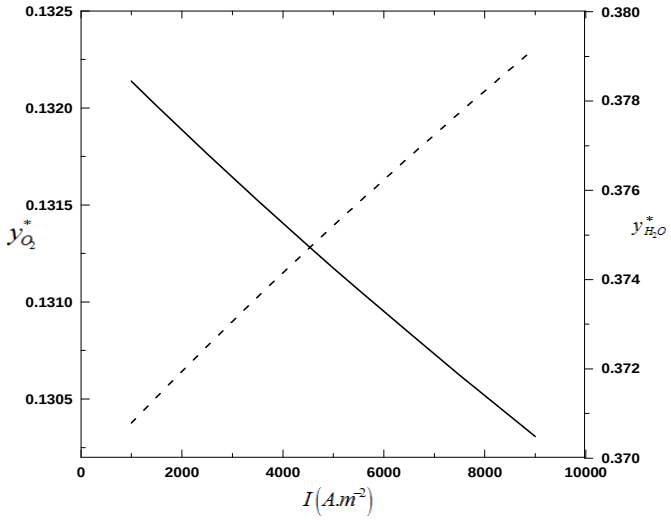

Figure 5. Oxygen and water mole fractions variation with current densities at cathode/membrane interface

3.3. Fuel cell performances

Polarisation curves with different cell temperature are shown in Figure 6. It is found that the performances of the fuel cell increases with the increases of the cell temperature. Indeed, the exchange current density increases with the increase of fuel cell temperature, which reduces activation losses. Another reason for the improved performances is that higher temperatures improve mass transfer within the fuel cells and leads to net decrease in cell resistance. In fact, a higher temperature significantly reduces the activation overpotential and greatly raises the oxygen concentration at the reaction sites due to the increase of the activation of the electrochemical reaction at the membrane/cathode interface.

The shifting of the polarization curves towards higher voltage at higher current densities when increasing the cell temperature is due to the increase of conductivity of the membrane. The maximum power density shifts towards higher current density with an increasing temperature as a result of reduced ohmic loss.

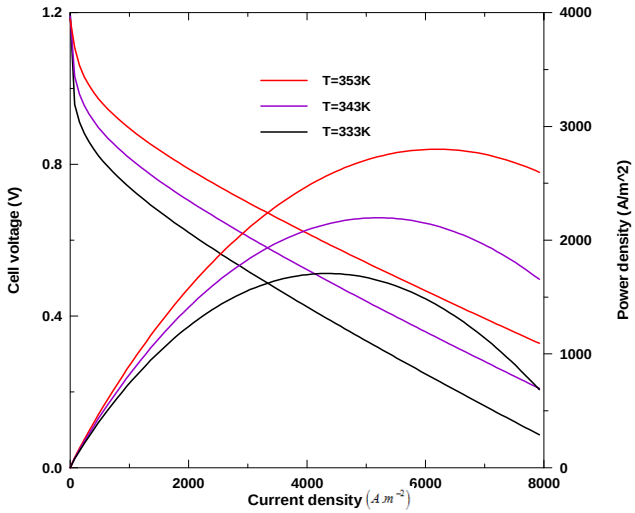

Figure 6. Cell performance for different cell temperature

As depicted by figure 7, the performances of the fuel are enhanced with high humidity. The curve is more ameliorated when both gas streams are humidified due to the higher membrane hydration. For the remaining two situations (RHa=80%, RHc=20% and RHa=20%, RHc=80%), there is no significant difference between curves for these operating conditions. The differences between the polarization curves are more evident for the higher values of current density, since the electro-osmotic drag also increases. For these conditions the anode stream humidification becomes more relevant.

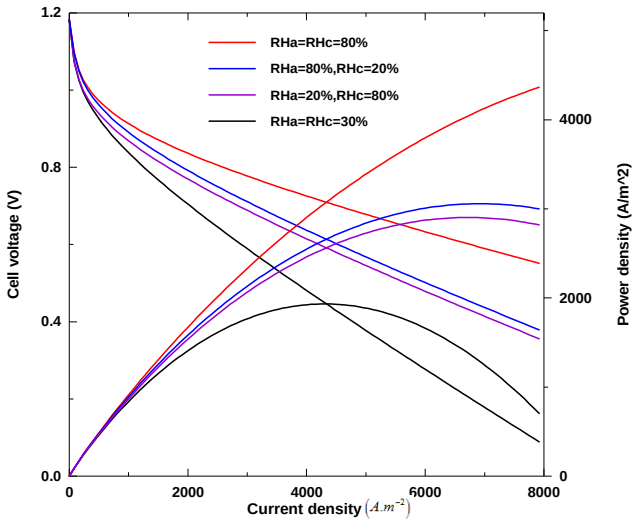

Figure 7. Cell performance for different operation conditions

Figure 8 shows that the performance of the fuel cell improves with the increase of pressure. The overall polarization curves shift positively as the pressure increases. The reason for the improved performances is that the partial pressure of the reactant gases with increasing operating pressure increases.

The maximum power improves by increasing pressure because of the rate of the chemical reaction which is proportional to the partial pressures of the hydrogen and the oxygen. Thus, the effect of increased pressure is most prominent when using air. Higher pressures help to force the hydrogen and oxygen into contact with the electrolyte. This sensitivity to pressure is greater at higher current densities.

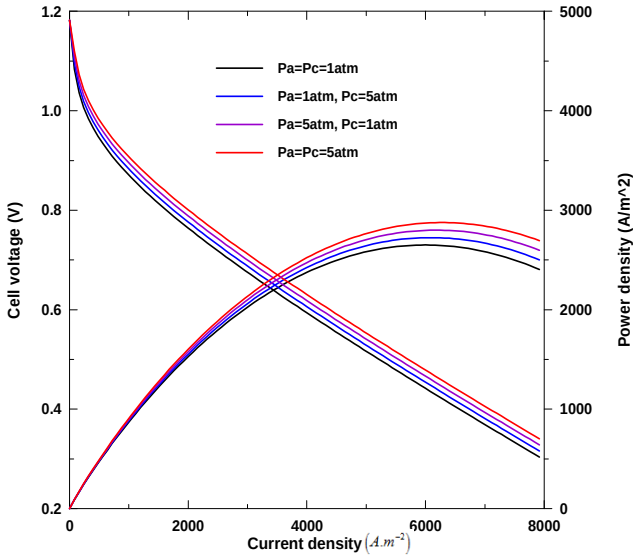

Figure 8. Cell performance for different operation pressure

4. CONCLUSION

A comprehensive model which takes in to account many processes, namely, species transport in the porous electrodes, water transport in the membrane and the electrochemical reactions in the active areas, is implemented in this study. The effect of operating conditions on the PEMFC performances is investigated. From this study, we can conclude:

1/ Temperature plays a key role in the activation of the electrochemical reaction at the cathode/membrane interface and then, on oxygen consumption. The performance of the fuel cell increases with the increases of the cell temperature. In fact, the exchange current density increases with the increase of fuel cell temperature, which reduces activation losses.

2/ the maximum power shifts positively with an increasing pressure because of the rate of the chemical reactions which is proportional to the partial pressures of the hydrogen and the oxygen. Cathode pressure is more effective to the fuel cell performance than anode pressure.

3/ the fuel cell performances are more ameliorated when both gas streams are humidified due to the higher membrane hydration.

REFERENCES

[1] Bernardi D M, Verbrugge M W. A mathematical model of the solid-polymer-electrolyte fuel cell. *J. Electrochem. Soc.*, vol 139, pp. 2477-2491, 1992

[2] Springer T E, Zawodzinski T A, Gottesfeld S. Polymer electrolyte fuel cell model. *J. Electrochem. Soc.*, vol 138, pp. 2334-2342, 1991

[3] Amphlett JC, Baumert RM, Mann RF, Peppley BA, Roberge PR, Harris TJ. Performance modeling of the ballard mark IV solid polymer electrolyte fuel cell. *J Electrochem Soc.* Vol 142, pp. 1-8, 1995

[4] Prodip K. Das, Xianguo Li, Zhong-Sheng Liu, Analysis of liquid water transport in cathode catalyst layer of

PEMFCs. *Int. J. of Hydrogen Energy*, vol 35, pp. 2403-2416, 2010

[5] Najjari, M., Khemili, F. and Ben Nasrallah, S., The effects of the cathode flooding on the transient responses of a PEM fuel cell. *J. Renewable Energy*, vol 33, pp. 1824-1831, 2008

[6] Khemili, F, Najjari, M., Ben Khadher, N and Ben Nasrallah, S., Two-dimensional modelling of Transport phenomena by (CVFE) method in the porous cathode of a PEM fuel cell . *J. of Porous Media*, vol 12, pp. 1305-1317, 2009.

[7] A tow-dimensional, transient and isothermal model for the air cathode of PEM fuel cells, *Int. J. Heat and Technology*, article in press.

[8] Kim J, Lee S-M, Srinivasan S, Chamberlin CE. Modeling of proton exchange membrane fuel cell performance with an empirical equation. *J Electrochem Soc.*, vol 142, pp. 2670-2674, 1995.

[9] Lee JH, Lalk TR, Appleby AJ. Modeling electrochemical performance in large scale proton exchange membrane fuel cell stacks. *J Power Sources*, vol 71, pp. 258–68, 1998.

[10] Korsgaard AR, Refshauge R, Nielsen MP, Bang M, Kær SK. Experimental characterization and modeling of commercial polybenzimidazole based MEA performance, J. *Power Sources*, vol 162, pp. 239-245, 2006.

[11] M.G. Santarelli , M.F. Torchio, P. Cochis. Parameters estimation of a PEM fuel cell polarization curve and analysis of their behavior with temperature. *Journal of Power Sources*, vol 159, pp. 824-835, 2006.

[12] Hyunchul Ju, Hua Meng, Chao-Yang Wang, A single-phase, non-isothermal model for PEM fuel cells, *Int. J. of Heat and Mass Transfer*, vol 48, pp. 1303-1315.

[13] Sophie Didierjeana, Olivier Lottin, Gael Maranzana, Thierry Geneston, PEM fuel cell voltage transient response to a thermal perturbation. *J. Electrochimical Acta*, vol 53, pp. 7313-7320, 2008.

[14] K.T. Jeng, S.F. Lee, G.F. Tsai, C.H. Wang. Oxygen mass transfer in PEM fuel cell gas diffusion layers. *Journal of Power Sources*, vol 138, pp. 41-50, 2004.

[15] T.A. Zawodzinski, T.E. Springer, J. Davey, R. Jestel, C. Lopez, J. Valerio, S. Gottesfeld, A comparative study of water uptake by and transport through ionomeric fuel cell membranes, *J. Electrochem. Soc.*, vol 140, pp. 1981-1985, 1993.

[16] J.T. Hinatsu, M. Mizuhata, H. Takenaka, Water uptake of perfluorosulfonic acid membranes from liquid water and water vapor, *J. Electrochem. Soc.*, vol 141, pp. 1493-1498, 1994.

[17] Berning T, Djilali N. Three-dimensional computational analysis of transport phenomena in a PEM fuel cell-a parametric study. *J Power Sources*, 124, pp. 440-452, 2003.